Vol 10 Suppl., July 2001
1009-1963/2001/10(Suppl.)/S100-08

Chinese Physics

© 2001 Chin. Phys. Soc.
and IOP Publishing Ltd

# IDENTIFICATION OF MEMBRANE PROTEINS IMAGED BY ATOMIC FORCE MICROSCOPY USING A TEMPLATE MATCHING ALGORITHM

Oliver Enders[a], Enrico Martinoia[b], Carsten Zeilinger[a], and Hans-Albert Kolb[a]

[a] *Institute of Biophysics, University of Hanover, Herrenhäuser Str.* 2, D-30419 *Hannover*

[b] *Institut de Botanique, Laboratoire de Physiologie Végétale, Rue Emile-Argand* 13, CH-2007 *Neuchatel*

(Received 2 December 2000; revised manuscript received 19 March 2001)

The atomic force microscope allows to image biological samples in their native environment. But the identification and the topography of individual randomly distributed membrane proteins is still a challenge. We used membranes of isolated vacuoles of barley mesophyll cells. Images at low resolution indicate that vacuoles spontaneously attach, rupture and finally adsorb completely as planar membrane to mica. Height profiles indicate that the membrane at the peripheral boundary exposes the extravacuolar surface to the scanning tip. At molecular resolution a template matching correlation algorithm was used to identify the most abundant membrane protein, the vacuolar $H^+$-ATPase by the characteristic extravacuolar head of the transport molecule. The data indicate the possibility to analyse single randomly distributed membrane proteins in their native environment with the knowledge of a suitable template.

**Keywords:** atomic force microscope, vacuolar membrane, $H^+$-ATPase, template matching
**PACC:** 6116P, 8265

## I. INTRODUCTION

The atomic force microscope (AFM)[1] has become a powerful tool to image biological structures ranging from whole cells to substructures and single biomolecules.[2−4] One of the major advantages of atomic force microscopy is the possibility to image the samples in physiological fluids at adjusted ionic strength and electrolyte composition.

Biological membranes are soft and therefore have to be firmly attached to a solid support to allow images by AFM to molecular resolution. Native biological membranes are usually associated with peripheral networks like the cytoskeleton, which either lead to a soft support of the membrane and thereby reduce the resolution significantly[2,5] or hinder the direct access of the scanning tip to the membrane surface. It is therefore desirable to use native biological membranes, which do not have to be reconstituted, but spontaneously form smooth planar membrane patches on solid surfaces. To match these requirements we selected isolated vacuoles, since the vacuolar membrane, the tonoplast, is not associated with a cytoskeleton. Intact vacuoles can be isolated within a few hours,[6,7] thus allowing an investigation by AFM without intermediate freezing and thawing for storage reasons.

Applying AFM either in contact or tapping mode, single membrane molecules could be identified and even resolved to the level of molecular substructures by use of algorithms of averaging, if the proteins were ordered in a quasi-crystalline pattern in the membrane.[8−10] The unambiguous identification of individual randomly distributed membrane proteins within the native membrane can be achieved by using the adhesion mode. For this mode the tip of the AFM is functionalised with specific biological or chemical molecules to measure the adhesion force between the specific molecules at the tip and the sample.[9,11−16] However, although single molecules can be identified, their submolecular topography has not been resolved so far.

In the present paper we show that in the case of supported vacuolar membranes the membrane topography can be analysed to nanometer resolution. In addition, it was possible to identify the characteristic cytoplasmic head group of the major integral membrane protein, the vacuolar $H^+$-ATPase.[17] For this purpose we used known structural models of the vacuolar $H^+$-ATPase based on electron micrographs[18] and for the first time applied a template matching algorithm to improve the identification of individual specific membrane proteins in AFM images. This correlation based template matching algorithm is well known in image processing science and is part of the so called correlation averaging method, which is applied to increase the signal to noise ratio of structures under investigation in electron micrographs[19] or AFM images of crystal like biological structures.[8] The presented data indicate, that the application of the template matching method supports the identification of individual

proteins by AFM within a soft environment of randomly distributed membrane protrusions of different size and shape.

## II. MATERIALS AND METHODS

### A. Plant material and vacuole isolation

Barley seedlings (Hordeum vulgare L. cv. Baraka, Serasem, France) were grown at 23°C (day) and 16°C (night) at 60% humidity in a growth chamber using Phillips Powerstar HQI-400 W/N as a light source with a 16 h photoperiod. Protoplasts were prepared from primary leaves as described by Ref.[6]. Vacuoles were isolated according to Ref.[7], however Bovine Serum Albumine (BSA) was omitted from the solutions. Pectolyase and Cellulase were purchased from Seishin Corp. Tokyo, Japan. Buffers, percoll and salts were delivered by Sigma-Aldrich, Germany and Roth, Germany. All buffer solutions were stored on ice before usage. Protoplasts and vacuoles were isolated and held at 4°C.

### B. Mica preparation

Pieces of about 2×2mm mica fragments were cut and fixed bubble free by a two-component adhesive (Sylgard, Dow Corning Corp.) at 100°C on glass cover slips. Impurities were removed by incubation with a 2% tenside solution of Hellmanex II (Hellma GmbH) in $H_2O$, for 30min. The slides were washed with bidestilled $H_2O$ (Milli-Q plus), dried and stored dust-free. The mica surface was freshly cleaved by mounting and carefully removing an adhesive strip prior to the addition of the vacuole suspension. About 10$\mu$l of the vacuole suspension was placed on freshly cleaved mica and incubated 2h at 4°C. Evaporation was avoided by adding a reservoir of buffer solution in a sealed container during incubation. After incubation the cover slip was rinsed extensively with about 20 ml of sorbitol buffer solution and immediately transferred to the fluid chamber of the AFM. To minimise thermal drift during the scan process, all buffer solutions were kept at room temperature before usage for at least 1h.

### C. Atomic force microscopy

An atomic force microscope Nanoscope IIIa/Multimode (Digital Instruments (DI), Santa Barbara, USA), equipped with a 120 $\mu$m-scanner and a fluid cell was used. All parts of the fluid cell were cleaned with ethanol and rinsed in bidestilled $H_2O$. The o-ring seal of the fluid cell was cleaned with isopropyl alcohol. To maintain the activity and the native structure of the proteins, scanning was performed in the sorbitol buffer. All images were acquired using $Si_3N_4$-tips (Olympus OMCL-TR800 PSA, spring constant 0.16N/m, resonance frequency 27kHz ,tip radius 20nm). The cantilevers were incubated in 2% tenside-solution for at least 20 min and rinsed extensively with water before mounting into the fluid cell. To avoid thermal bending of the cantilever and thus to ascertain a constant imaging force, the experiments were started about 1.5 hrs after setting up all components for thermal equilibration.

Prior to the scanning process the photo detector response was calibrated by a force distance curve on bare mica surface following the instructions given by the manufacturer of the instrument. The quality of each tip was tested by scanning images of the bare mica surface with atomic or lattice resolution. All data were acquired in contact mode or with oscillating cantilever ('tapping-mode$^{TM}$'). The scan speed was selected to 1–50$\mu$m/s in order to avoid a significant lateral drift between sample holder and cantilever. The parameters of the z-controller were set to 'constant-force-mode', to maintain an imaging force well below 1nN in contact mode. In tapping-mode, the oscillation frequency was set to the eigenfrequency of the cantilever. The set point of the oscillation amplitude was tuned to 70% to 90% of the free oscillation amplitude, to minimise image distortion by the scanning process and to obtain stable imaging conditions.

### D. Off-line processing

Topographical data were corrected by the error signal, to rule out topographical artefacts due to time delays of the feedback loop. The error signal was calibrated with the sensitivity of the photo detector response which was obtained from force calibration curves on bare mica (see above).

Effects of scan axis coupling and slow thermal drift on the topographical data in z direction were corrected by applying the 'plane fit' algorithm of the instruments image processing software. In order to improve the evidence for the presence of individual vacuolar $H^+$-ATPase molecules, high resolution images of the vacuolar membrane were analysed with a correlation template matching algorithm. The calculated correlation map indicates positions with high spatial similarity to the modelled vacuolar $H^+$-ATPase. The numerical correlation analysis was conducted with the

visualisation package AVS on a SGI Onyx graphic workstation and visualised by AVS/Express.

### E. Estimation of the Tip Radius

The true radius of the scanning tip is an essential parameter for the geometrical estimation of the topography. In order to consider the specific experimental conditions, the tip radius was estimated from data of the respective series of experiments. Since within the presented experiments, membrane sheets were imaged, the height profiles of membrane patches were used to estimate the actual tip radius. The tip broadening effect caused the border of the imaged membrane patch to be 'smeared out' laterally. This effect can be simulated geometrically as illustrated in Fig.1(a). The figure shows a spherical tip, which is moved 'in contact' across a modelled membrane boundary.

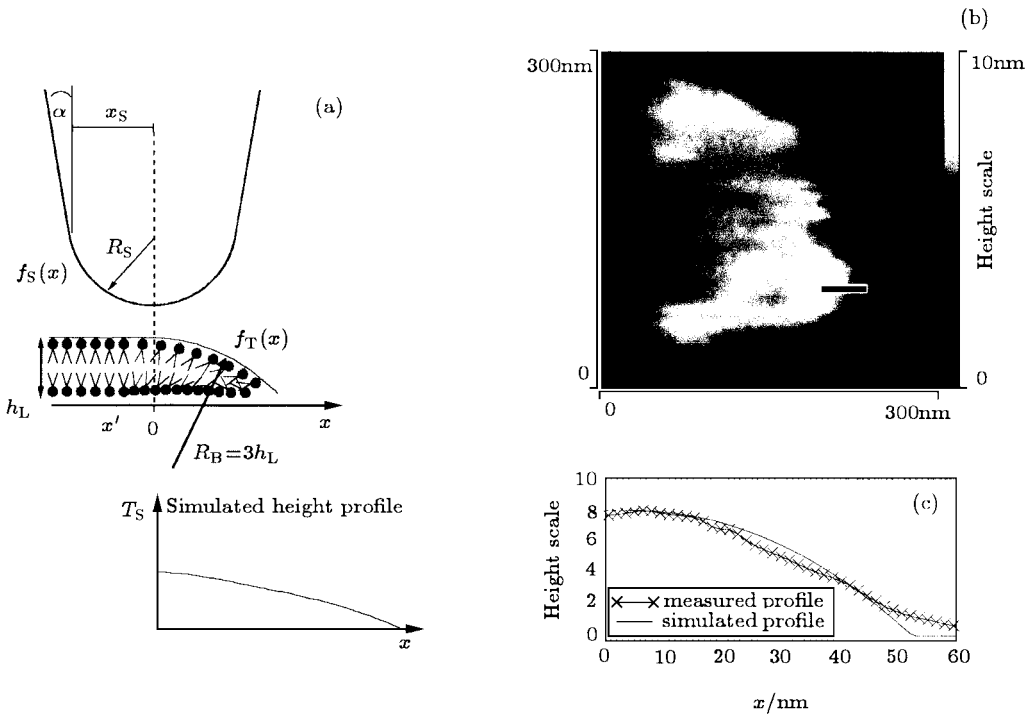



**Fig.1.** (a) One dimensional simulation of the tip broadening effect at the rim of a membrane adsorbed to mica. $f_T(x)$ represents the surface profile of an adsorbed membrane, $f_S(x)$ represents the tip profile and $T_S(x)$ shows schematically the generated actual profile including the tip broadening effect. (b) Example of topography obtained in contact mode of the boundary region of a vacuolar membrane sheet. The black bar indicates the section of the scan line, which was taken to simulate the recorded height profile by $T_S(x)$. (c) Both the recorded height profile and the best fit for $T_S(x)$ are presented. The fit of $T_S(x)$ gives an estimate of $f_S(x)$ and therefrom the tip radius could be derived.

### F. Correlation template matching

The one dimensional height profile of the membrane boundary $f_T(x)$ is described as a circular function of the horizontal parameter $x$ with a radius $R_B$ estimated to be 3 times larger than the thickness of a bilayer $h_L$:

$$f_T(x) = \left\{ \begin{array}{lll} h_L & x < 0 & \\ \sqrt{R_B^2 - x^2} - (R_B - h_L) & x \geq 0 & \text{and } x \leq \sqrt{R_B^2 - (R_B - h_L)^2} \\ 0 & \text{otherwise} & \end{array} \right\} \quad (1)$$

The tip is described as a cone with spherical tip:

$$f_S(x) = \left\{ \begin{array}{ll} \cot(\alpha)(x - x_S) - R_S \sin(\alpha) & x \in ]-\infty, x_S] \\ -R_S \sqrt{1 - \left(\frac{x}{R_S}\right)^2} & x \in ]-x_S, x_S[ \\ -\cot(\alpha)(x + x_S) - R_S \sin(\alpha) & x \in [x_S, \infty[ \end{array} \right\} \quad (2)$$

$\alpha$ denotes the opening angle of the cone. $x_S$ defines the transition point between sphere and cone:

$$x_S = R_S \cos(\alpha) \tag{3}$$

The simulated topography can be calculated by:

$$T_S(x) = \max\{x' | f_S(x' - x) - f_T(x')\} \tag{4}$$

The output of the simulation yields a two-dimensional curve resembling the height profile of a membrane boundary which was broadened by the finite tip radius (Fig.1(c)). The actual value of the tip radius was estimated by variation of the tip radius in the simulation until the deviation of the simulated curve to the experimental cross section was minimal.

Correlation template matching is an image processing method, which was derived from a relation of statistical mathematics, describing the statistical dependence of two variables. The latter is known as correlation coefficient. Applied to image processing, the correlation coefficient describes the spatial similarity between two images. The correlation coefficient ranges from –1 to 1, where 0 means no similarity, –1 indicates, that the compared images are inverted and +1, that the images are identical. If special image features have to be recognised, a 'template' image representing the feature of interest is 'convolved' with the image. For this algorithm, the correlation coefficient between the template image and each 'window' of the original image of comparable size is calculated. With the two-dimensional correlation coefficient:[20]

$$\gamma(x_0, y_0) = \frac{\sum_{x,y}^{max_s} (b_{x+x_0, y+y_0} - \overline{b}_{x_0,y_0})(s_{x,y} - \overline{s})}{\left\{ \sum_{x,y}^{max_s} (b_{x+x_0,y+y_0} - \overline{b}_{x_0,y_0})^2 \right\} \left\{ \sum_{x,y}^{max_s} (s_{x,y} - \overline{s})^2 \right\}} \tag{5}$$

a map is obtained describing the spatial similarity between the template topography ($s_{x;y}$) and the rectangular detail of the original image ($b_{x+x_0,y+y_0}$). ($x_0$, $y_0$) denotes the variable offset of the latter within the original image. $\overline{b}_{x_0,y_0}$ gives the average topographical height of the rectangular detail as function of ($x_0$, $y_0$). s gives the average height of the template. $max_s$ describes the maximum number of pixel per row (respectively per column) of the template. High values of $\gamma(x_0, y_0)$ indicate those coordinates ($x_0$, $y_0$), where the template matches the original image.

If this method is applied to the recorded image, an appropriate template has to be acquired. We used a template image which was generated from a model of the cytoplasmic part of the vacuolar $H^+$-ATPase.[21] Since the resolution of the recorded images was not sufficient to identify subunits of membrane proteins, the template was numerically generated by a simple one-dimensional simulation of the scan procedure of the head and stalk of the vacuolar $H^+$-ATPase. The latter was modelled as a box function with a height of 14nm and a width of 10nm. The derived one dimensional profile of the head included the height given by the stalk and the broadening effect due to the finite radius of the tip. The profile was extended to two dimensions assuming a rotational symmetry of the head and the tip. Finally, the template was resampled according to the resolution of the original image.

## III. RESULTS

### A. Membrane topography at micrometer scale

After isolation of vacuoles from barley leaves, a drop of vacuole suspension was placed on freshly cleaved mica and incubated for 1 to 14h. Figure 2 shows a representative topography at micrometer scale, which was measured in tapping mode.

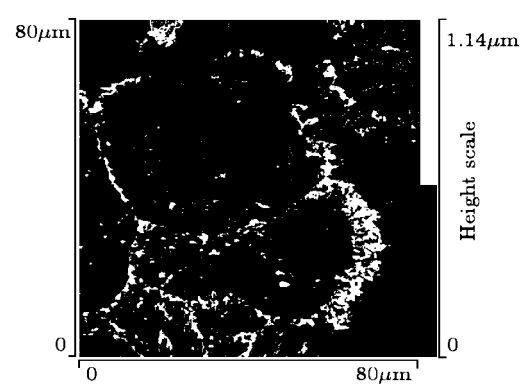



**Fig.2.** Topography of single vacuolar membranes adsorbed to mica. Different membrane areas can be clearly distinguished as described in section Results. The scan was acquired in tapping mode with a driving frequency of 31 kHz. The amplitude set point was adjusted to about 80% of the free oscillation amplitude. 256 lines with 512 samples/line were scanned at a rate of about 1 scan line/s.

Adsorbed and spread vacuoles can be identified. Adsorbed membrane areas can be easily discriminated. A circular central area of lower protrusion density compared to that of the surrounding intermediate area is visible. Finally, a circular area with numerous radial oriented clefts surrounds the intermediate area and forms the rim or peripheral area of adsorbed vacuoles. The figure indicates that the peripheral membrane became fragmented to membrane lobes by a folding process during the adsorption process and is piled up to a second membrane layer.

In the following, height profiles of adsorbed vacuoles will be used to elucidate the orientation of the adsorbed membrane at the outer boundary. For the height difference between the surface of the fragmented membrane lobes of the peripheral area and the intermediate surface area a value of 8.0±0.6nm was determined. Corresponding height profiles in both areas show that the majority of protrusions has a height between 4nm and 12nm. Some protrusions have a height between 13nm and 15nm. Only a few protrusions heigher than 16nm could be observed (see also Figs.3, 4).

As outlined in the discussion part, the data give evidence that the topography of the upper layer of the peripheral area exposes the extra vacuolar or cytoplasmic membrane surface. Following this suggestion we tried to identify the vacuolar $H^+$-ATPase by exploring the height and topography of the cytoplasmic oriented head group.

### B. Identification of the extravacuolar head of the vacuolar $H^+$-ATPase molecule

Without further fixation the fragmented upper layer at the peripheral area was imaged in contact and tapping mode. The recordings were performed in buffer conditions, which maintain the enzymatic activity of vacuolar $H^+$-ATPases . It turned out that for images at high resolution with low sample distortions, used tips yielded the best results. The tip radii $R$ were estimated to be in the order of 100nm. This size is in accordance with models of a tip sample interaction, which indicate that a sharp tip ($R$ <10nm) does not necessarily provide highest resolution.[2]

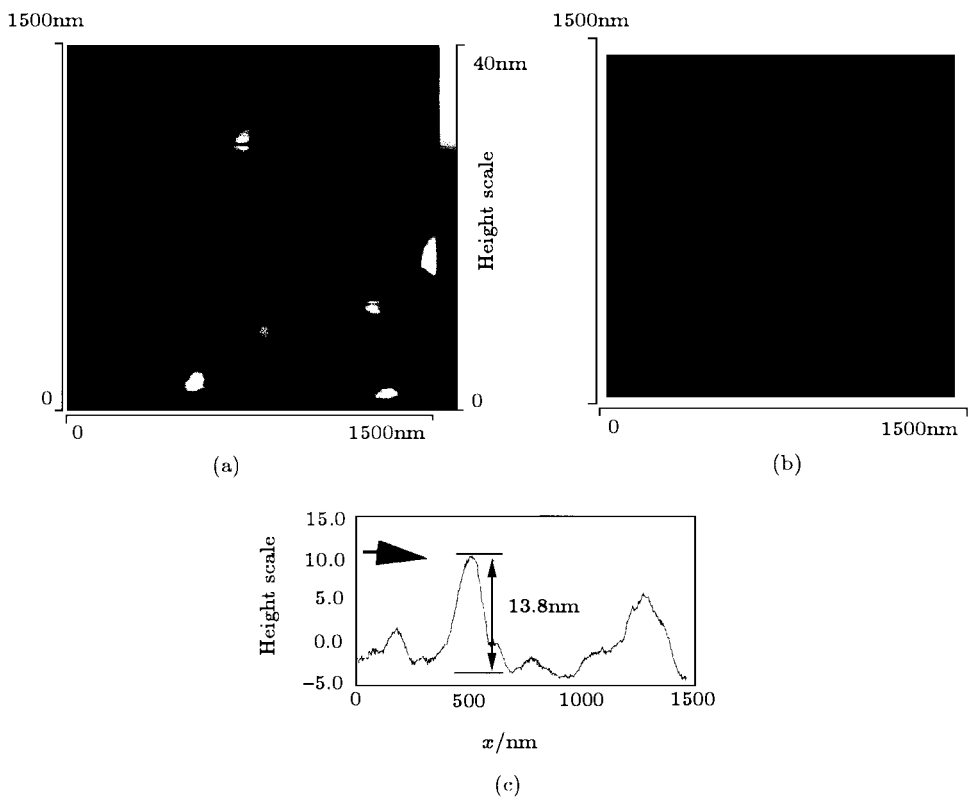



**Fig.3.** (a) Image of a membrane fragment at the peripheral area in contact mode. Some protrusions have a height of about 14nm above the membrane surface. (b) Plot of the correlation coefficient of a template generated from the cytoplasmic part of the vacuolar $H^+$-ATPase with the data shown in (a). Yellow spots indicate a correlation coefficient larger than 0.7 and red spots of above 0.8. Protrusions with geometrical heights in the order of 14nm correspond to a high correlation coefficient. Image (a) consists of 512 scan lines acquired with a scan rate of 6 lines/s. The imaging force was adjusted to about 0.5nN. (c) Height profile along a selected scan line as indicated in (a).

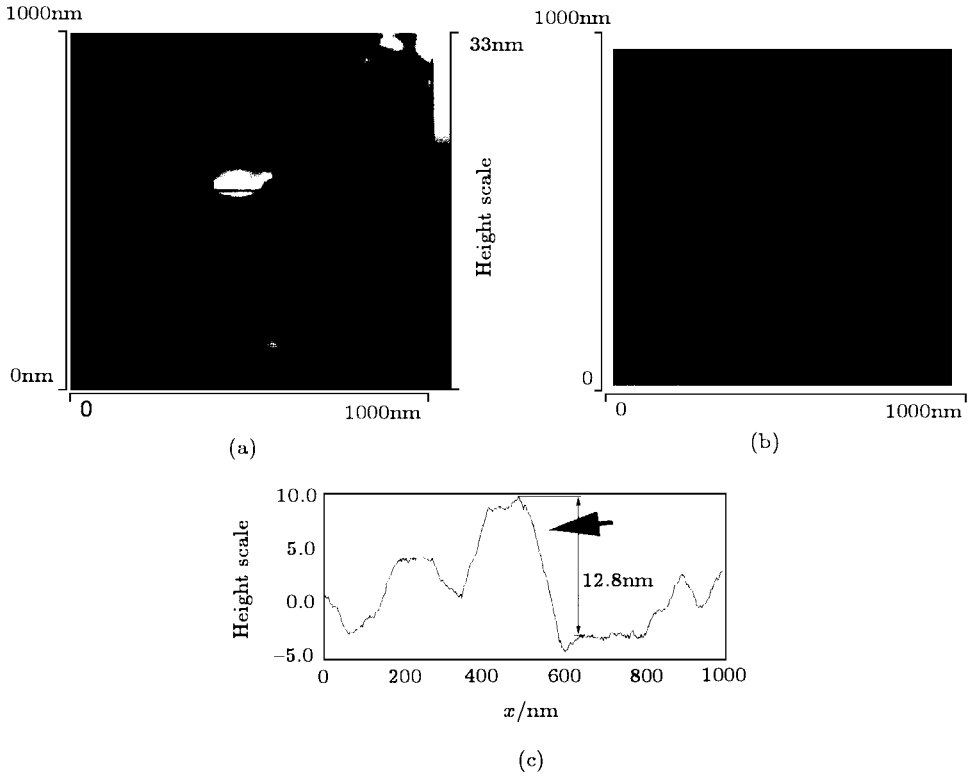



**Fig.4.** (a) Image of a membrane fragment at the peripheral area in tapping mode. (b) plot of the correlation coefficient. Yellow spots indicate a correlation coefficient larger than 0.7 and red spots of more than 0.8. Correlation coefficients and protrusion heights appear to be lower than those obtained in contact mode (compare with Fig.3), (c) Height profile along the scan line indicated in (a). In tapping mode the cantilever oscillated with an amplitude of about 100nm and the damped amplitude was 90% of the free oscillation amplitude.

Figures 3(a) and 4(a) show high resolution images of a fragmented membrane lobe in contact mode. Randomly distributed protrusions are visible.

From the corresponding topography profile height values of 13nm to 14nm were found for some protrusions (see Fig.3(c) and Fig.4(c). In comparison, the image recorded in tapping mode (Fig.4(a)) appeared to be less distorted by the tip sample interaction (compare to Fig.3(a)). In tapping mode a higher resolution could be achieved, i.e. the smallest distinguishable protrusions were about 20% smaller in diameter in contact mode than in tapping mode. However the height of protrusions in the order of 14nm appeared to be about 1nm smaller than in contact mode. But for both imaging modes the apparent diameter of those protrusions was about 200nm.

In order to support the assumption that protrusions with a height of 13nm to 14nm represent cytoplasmic oriented heads of the vacuolar $H^+$-ATPase, a correlation template matching algorithm was applied. For application of this algorithm the images of Fig.3(a) and Fig.4(a) were matched with a modelled image of the extra vacuolar head of vacuolar $H^+$-ATPases.[18] The result is presented as two dimensional map of a correlation coefficient $\gamma(x, y)$. Regions of high correlation are colored yellow ($\gamma(x, y) > 0.7$) and red ($\gamma(x, y) > 0.8$). Figures 3(b) and 4(b) indicate, that protrusions with a geometrical height of about 13nm to 14nm are related to a correlation coefficient above 0.7.

## IV. DISCUSSION

The present work introduces mica supported vacuoles of barley leaves as a promising system to analyse the extravacuolar topography of individual randomly distributed membrane proteins by atomic force microscopy in their native environment.

In the following the adsorption process and the orientation of the adsorbed vacuolar membrane is discussed. Since vacuoles are free of cytoskeletal structures, they resemble giant lipid vesicles or liposomes. Therefore the observed adsorption process can be described in terms of models applied for vesicle adhesion and consecutive bilayer formation.[22–30]

At the peripheral area, membrane sheets are visible, which do not adsorb to the mica surface, but

form a second layer on top of the underlying membrane sheet. This finding is supported by the measured height profile and has not been observed for vesicles or liposomes. We suggest, that the membrane lobes of the peripheral area expose the extravacuolar face to the scanning tip.

### Images at molecular resolution

The aim of this work was to acquire images of the vacuolar $H^+$-ATPase *in situ*. As outlined above, the membrane fragments seen at the borderline of the adsorbed vacuoles provide access to the extravacuolar side of the membrane. For an identification of vacuolar $H^+$-ATPase three molecular parameters are considered which are already known from electron micrographs of negatively stained or freeze fractured surfaces of vacuolar membranes.[18] The parameters are the height and diameter of the head and stalk structure of vacuolar $H^+$-ATPase pointing out of the membrane. Protrusions with heights between 12nm and 15nm were found in tapping mode (see Fig.4(a)) and in contact mode (see Fig.3(a)). It should be noted that in contact mode height values can be considered as unbiased. The observed values are in reasonable agreement with the corresponding value of about 14nm derived by electron microscopy.[21] However, the apparent diameter of about 200nm for these protrusions appears to be significantly larger than the expected value of about 20nm. The discrepancy can be explained by the influence of the tip broadening effect in AFM-images.[2] The effect depends on both the radius and height of the imaged structure. An estimate of the tip radius yields a value in the order of 100nm. Using this tip radius and a function which describes the cytoplasmic part (head and stalk) of the vacuolar $H^+$-ATPase a template can be generated. By application of the template matching algorithm correlation coefficients above 0.7 were calculated for protrusions with a height of about 14nm. This finding gives evidence for the presence of vacuolar $H^+$-ATPase in the peripheral membrane area of AFM-images. Furthermore, considering the diameter of the pronounced protrusions, it has to be expected that the lateral mobility of the protein head affects the derived diameter. Since the head is connected by a flexible stalk to the integral membrane subunits, it could be moved or swerved by the scanning tip, thus enlarging the expected lateral dimensions. The data indicate the possibility, to identify individual membrane proteins like the vacuolar $H^+$-ATPase with the knowledge of a corresponding template.

### ACKNOWLEDGEMENT

The technical support of Dipl. Phys. R. Schauer is gratefully acknowledged.

## References

[1] Binning G, Quate C F and Gerber C 1986 *Phys. Rev. Lett.* **56** 930
[2] Shao Z, Mou J, Czajkowsky D M, Yang J and Yuan J Y 1996 *Advances in Physics* **45** 1
[3] Müller D J, Fotiadis D, Scheuring S, Müller S A and Engel A, 1999 *Biophys. J.* **76** 1101
[4] Kolb H A, Enders O and Schauer R 1999 *Appl. Phys.* A **68** 247
[5] Beckmann M, Kolb H A and Lang F 1994 *J. Membr. Biol.* **140** 197
[6] Kaiser G, Martinoia E, Wiemken A 1982 *Z. f. Pflanzenphys* **107** 103
[7] Rentsch D, Martinoia E 1991 *Planta* **184** 532
[8] Müller D J, Büldt G and Engel A 1995 *J. Mol. Biol.* **249** 239
[9] Hansma P K, Cleveland J P, Radmacher M, Walters D A, Hillner P E, Bezanilla M, Fritz M, Vie D, Hansma H G, Prater C B, Massic J, Fukunaga L, Gurley J and Elings V 1994 *Appl. Phys. Lett.* **64** 1738
[10] Wiechmann M, Enders O, Zeilinger C and Kolb H A 2001 *Ultramicroscopy* **86** 159
[11] Florin E L, Moy V T and Gaub H E 1994 *Science* **264** 415
[12] Lee G U, Chris L A and Colton R J 1994 *Science* **266** 771
[13] Hinterdorfer P, Baumgartner W, Gruber H J, Schilcher K and Schindler H 1996 *Proc. Natl. Acad. Sci. USA* **93** 3477
[14] Dammer U, Hegner M, Anselmetti D, Wagner P, Dreier M, Huber W, Güntherodt H J 1996 *Biophys. J.* **70** 2437
[15] Schmitt L, Ludwig M, Gaub H and Tampe R 2000 *Biophys. J.* **78** 3275
[16] Willemsen O H, Snel M M E, Van der Werf K O, De Grooth B G, Greve J, Hinterdorfer P, Gruber H J, Schindler H, Van Kooyk Y and Figdor C G 1998 *Biophys. J.* **75** 2220
[17] Hedrich R, Kurkdjian A, Guern J and Flügge U 1989 *EMBO J.* **8** 2835
[18] Lüttge U, Ratajczak R, The physiology, biochemistry and molecular biology of the plant vacuolar ATPase. In Leigh A and Sanders D eds 1997 *The Plant Vacuole, Academic Press* New York, vol. 25, p 253
[19] Saxton W O and Baumeister W 1982 *J. Micr.* **127** 127
[20] Russ J C 1995 The Image Processing Handbook (CRC Press, Boca Raton) p 341

[21] Rockel B, Ratajczak R, Becker A and Lüttge U 1994 *J. Plant Phys.* **143** 318
[22] Seifert U and Lipowsky R 1990 *Phys. Rev.* A **42** 4768
[23] Nollert P, Kiefer H and Jähnig F 1995 *Biophys. J.* **69** 1447
[24] Vikholm I, Peltonen J and Tellman O 1995 *Biochim. Biophys. Acta* **1233** 111
[25] Feder T, Weissmüller G, Zeks B and Sackmann E 1995 *Phys. Rev.* E **51** 3427
[26] Xia Z and van de Ven T G M 1992 *Langmuir* **8** 2938
[27] Lipowsky R and Seifert U 1991 *Mol. Cryst. Liq. Cryst.* **202** 17
[28] Keller C A and Kasermo B 1998 *Biophys. J.* **75** 1397
[29] Beckmann M, Nollert P and Kolb H A 1998 *J. Membr. Biol.* **161** 227
[30] Rädler J and Sackmann E 1993 *J. Phys. II France* **3** 727